OPEN ACCESS Freely available online

Journal of
Membrane Science & Technology

Editorial

Simulation of Hollow Fiber DCMD Module for Desalination: Influence of Operating Conditions and Module Dimension

Sirisha Parvathaneni*

Department of Chemical Engineering, Indian Institute of Technology Delhi, New Delhi, India

ABSTRACT

The theoretical model for hollow fiber module for the process of direct contact membrane distillation is presented explicitly. The transport equations for the feed and permeate streams are simplified and are coupled with mass and heat transfer across the membrane. The resulting differential equations are discretized into n-number of steps and the flow variables; permeate flux was calculated for each step. In order to validate the model predictions with the experimental data; porosity (ε) and tortuosity (τ) are determined by using the Simplex Nelder-mead method. The influence of the inlet operating conditions and module dimensions of the module performance was analyzed. The effect of membrane length on the module performance showed a decreasing flux behavior after a certain increase in length due to decrease in the driving force across the membrane. The tradeoff between the permeate flux and performance ratio is analyzed for a different set of membrane parameters.

Keywords: Direct contact membrane distillation; Mathematical model; Simulation; Membrane parameters; Hollow fiber; Module performance

Abbreviations: J: Permeate flux ($kgm^{-2}h^{-1}$); M: Molecular weight ($kgmol^{-1}$); C_p: Specific heat ($J\ mol^{-1}\ K^{-1}$); T: Temperature (K); K: Thermal conductivity coefficient ($wm^{-1}K^{-1}$); H: Convective heat transfer coefficient ($wm^{-2}\ K^{-1}$);

D: Diameter(m); X: Mole fraction; V: Velocity (ms^{-1}); S: salt; W: water; F: feed side; P: Permeate side; ρ: molar density ($molm^{-3}$); ρ: Density ($kg\ m^{-3}$); λ: Latent heat of water (Jkg^{-1})

INTRODUCTION

Membrane Distillation (MD) is a thermally driven membrane separation process in which feed and permeate streams present are separated by the hydrophobic membrane. Only water vapor molecules or other volatile molecules transport through a hydrophobic membrane. The temperature gradient present between the vapor-liquid interfaces creates a vapor pressure difference across the membrane that acts as a driving force for the MD process. Such an MD process yields highly purified permeate and has wide applications for separating contaminants from liquid solutions. MD has significant advantages over other separation processes like Multi-Effect Distillation (MED); Reverse Osmosis (RO). MD can be operated at low temperature and pressure and requires less space when compared to MED and also results in 100% theoretically salt rejection [1]. For such advantages; MD is considered as the upcoming desalination technology for producing fresh water from seawater and for other applications [2-4]. Nevertheless; in the MD process; the high conductive heat loss through the membranes results in lower thermal efficiency. To overcome this disadvantage; research work has been carried out on the various heat recovery concepts [5,6]. For long term and efficient operation of MD; the process can be carried out with low grade and sustainable energy sources such as solar; wind; and geothermal energy using hybrid strategies such as coupling the process of MD with RO and developing new membrane manufacturing technologies and process design for MD [7,8]. However; a trade-off exists between the achievement of high flux and high thermal efficiency; which needs to be optimized.

One of the major drawbacks of the MD process over RO is the less permeate flux in case of MD. Hollow fiber modules for MD can be considered to provide high flux. This can be achieved by having high packing density of fibers which provides high surface area per unit volume. In literature; the models for Direct Contact Membrane Distillation (DCMD) in the hollow fiber module

Correspondence to: Sirisha Parvathaneni, Department of Chemical Engineering, Indian Institute of Technology, Hauz Khas, New Delhi-110016, India, E-mail address: Sirisha.p1991@gmail.com

Received: September 27, 2021; **Accepted:** October 13, 2021; **Published:** October 19, 2021

Citation: Parvathaneni S (2021) Simulation of Hollow fiber DCMD Module for Desalination: Influence of Operating Conditions and Module Dimension. J Membr Sci Technol. 12:262.

Copyright: ©2021 Parvathaneni S. This is an open-access article distributed under the terms of the Creative Commons Attribution License; which permits unrestricted use, distribution; and reproduction in any medium; provided the original author and source are credited.

were developed by considering the dusty gas model [9-10]. The experimentally validated model can be used to analyze the effect module dimensions and flow rates of bulk streams along the length of the hollow fiber module; transmembrane temperature difference; and thereby the permeate flux.

In the present work; a mathematical model for Direct Contact Membrane Distillation (DCMD) in a hollow fiber module (tube side-feed flow) is presented explicitly. The model contains simplified transport equations coupled with the heat and mass transfer across the membrane. In order to validate the model with the experimental data in the literature the membrane parameters of porosity and tortuosity are adjusted for different inlet flow rates and the constant value of parameters is determined by the Simplex Nelder-Mead method. Later the simulation of the model is carried out and a stepwise solution of the model is presented. The variations of feed and permeate stream flow rates and temperature along the length of the module are illustrated and the sensitivity of the permeate flux to operating conditions and module dimensions is analyzed.

METHODOLOGY

Modeling of DCMD for hollow fiber module

The mathematical model presented in this work is based on Cheng, et al. [9]. The model for hollow fiber module is verified with the experimental data obtained from the literature [5]. The parameters of membrane in the membrane distillation coefficient are estimated. The following equations are obtained in terms of mole fraction; velocity; and temperature on feed and permeate sides after simplifying the transport equations presented in Cheng, et al. [9].

$$\frac{dx_s}{dz} = \frac{4Jd_o}{d_i^2 \overline{\rho_f}^2 v_f M_f [\frac{M_s}{\rho_s} - \frac{M_w}{\rho_w}(1-\frac{1}{x_s})]} \quad (1)$$

$$\frac{dv_f}{dz} = -\frac{4JM_w d_o}{d_i^2 \overline{\rho_f} x_s M_f \rho_w [\frac{M_s}{\rho_s} - \frac{M_w}{\rho_w}(1-\frac{1}{x_s})]} \quad (2)$$

$$\frac{dT_f}{dz} = -\frac{4}{v_f M_f \overline{\rho_f} C_{p_f} d_i^2}[h_f d_i (T_f - T_1) - Jd_o C_{p_f} T_f] \quad (3)$$

$$\frac{dv_p}{dz} = -\frac{4Nd_o J}{\rho_p (d_s^2 - Nd_o^2)} \quad (4)$$

$$\frac{dT_p}{dz} = \frac{4Nd_o (T_p J C_{pp} - h_p (T_2 - T_p))}{\rho_p C_{pp} v_p (d_s^2 - Nd_o^2)} \quad (5)$$

Model solution procedure: The procedure for simulating the hollow fiber module model is summarized as follows:

- The module is discretized into 'n' parts as shown in Figure 1. For feed; the initial flow rate; temperature; composition in terms of mole fraction are known (Eqs. 6-8). At the entering point j=1; Eqs. 6-8 are considered for feed side inlet operating conditions

$$v_f(0) = v_f^{in} \quad (6)$$

$$x_s(0) = x_s^{in} \quad (7)$$

$$T_f(0) = T_f^{in} \quad (8)$$

For the permeate side; the boundary values at j=1 are guessed (Eq. 9-10).

$$v_p(0) = v_p^{out} \quad (9)$$

$$T_p(0) = T_p^{out} \quad (10)$$

- The local permeate flux and variables for feed and permeate sides are calculated

At j=n; the calculated permeate temperature is compared with the actual inlet permeate temperature. The tolerance limit for the difference between these two values is set as $|T_p^{calculated} - T_p^{actual} < 10^{-6} T_p^{in}|$. If this value exceeded thetolerance limit; the guessed value of T_{in} is adjusted by 0.01; based on the sign of $T_p^{calculated} - T_p^{actual}$ and the calculations are repeated from j=1; till the tolerance limit is satisfied. Once the convergence criteria for temperature is met; then the permeate velocity at j=n is calculated and the tolerance limit is checked again for the velocity in the same manner as for the temperature. All the model equations are solved using MATLAB

The membrane parameters porosity (ε) and tortuosity (τ) were determined by using the experimental data considered from the literature [5]. Though these parameters (ε;τ) are given in literature; the tortuosity value is assumed [5]. The porosity is adjusted within the range of ε-0.05 to ε+0.05. The parameters estimation in order to fit the calculated and actual value is done by minimizing the objective function Eq.11 by Simplex Nelder-Mead method

$$Error(\varepsilon, \tau) = \sum_{b=1}^{m} \sqrt{(1 - \frac{J_{theo}}{J_{expt}})^2} \quad (11)$$

Where J is the permeate flux and the subscripts 'theo' and 'expt' denote the model predicted value and the experimental value. For the parameter estimation; the experimental results at different inlet flow rates (b=1 to m) are considered from the literature [5]. The characteristics of the membrane module considered in present work are given in Table 1. The initial guess value of porosity and tortuosity are 0.7 and 1.4 respectively.

The thermal efficiency of the hollow fiber DCMD process is analyzed from the Performance Ratio (PR); and it is expressed as:

$$PR = \frac{1}{L}\int_0^L \eta(z) dz \quad (12)$$

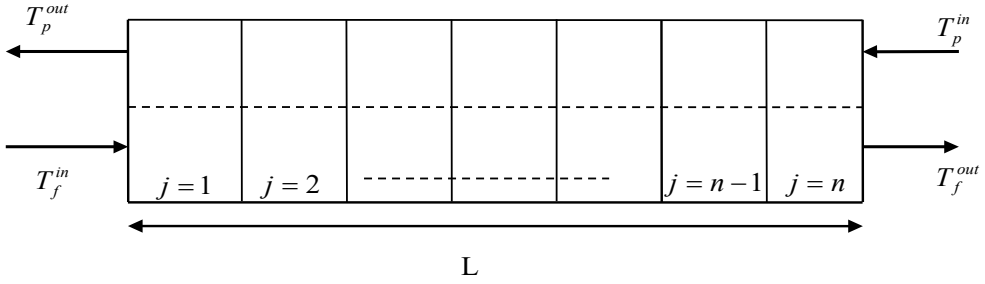

Figure 1: Discretization Hollow fiber module flow.

Table 1: Characteristics of hollow fiber membrane module.

Module material	PVDF
Length of the fiber; L (m)	0.45
Membrane thickness; δ (mm)	0.65
Nominal pore diameter (μm)	0.2
Fiber inner diameter; di (mm)	2.81
Fiber outer diameter; d0 (mm)	1.5
Number of fibers; Nf	40
Shell inner diameter; dsh (m)	0.021
Packing factor; ϕ	0.7
Surface area (m^2)	0.1

Where $\eta(z)$ is the local performance ratio and is defined as the ratio of the latent heat of vaporization (λ) of the transmembrane flux to the total heat transferred across the membrane. $\eta(z)$ is calculated by the following expression (Eq. 13).

$$\eta = \frac{J(z)\lambda}{J(z)\lambda + \frac{k_m}{\delta}(T_1(z) - T_2(z))} \quad (13)$$

Where $T_1(z)$ and $T_1(z)$ are the interfacial temperatures on the feed side and permeate side; respectively. k_m is the overall thermal conductivity of the membrane calculated using Eq. 14. Where ε is the membrane porosity. k_{po} and k_g refer to conductive coefficients of the vapor within the membrane pore and solid membrane respectively. k_{po} is calculated using Eq. (15); where $T_m = (T_1 + T_2)/2$.

$$k_m = (1-\varepsilon)k_{po} + \varepsilon k_g \quad (14)$$

$$k_{po} = 4.86\times10^{-4}T_m + 0.253 \quad (15)$$

From the performance ratio; the thermal efficiency of the process is estimated. Higher the performance ratio; lower are the heat losses due to conduction and results in higher thermal efficiency.

RESULTS AND DISCUSSION

The simulation of the model was carried out for aqueous NaCl solution at concentration of 35g/L. The performance of module is analyzed at different operating conditions and membrane characteristics. The inlet temperature of feed is varied from 323K to 343K; inlet temperature of permeate is varied from 288K to 303K; and the mass flow rate of feed stream is varied from 0.055 kg/s to 0.2 kg/s. The membrane thickness is also varied from 0.1 mm to 1 mm.

Model validation

The experimental data for the aqueous NaCl solution are listed in Table. 2. The measurements of the flux (J_v) at different v_f and T_f are used in the simulations to determine the unknown membrane parameters (ε and τ) using the Simplex Nelder-mead method in MATLAB. The predicted parameters are ε=0.73 and τ=1.8. Experimental and predicted flux for different feed inlet velocities are given in Table 2. The predictions are in reasonably good agreement with measurements. Further; the relative error between the predicted and measured J_v is calculated (E_{Jv}) (Table 2). It can be seen that the relative error between the experimental and theoretical values is ranging between -5.36% to +4.96%. As the relative error is small; the model can be considered to be appropriate for the description of DCMD in a hollow fiber module.

Influence of operating conditions on the performance of module

Effect of feed temperature: Figure 2 shows that as the feed inlet temperature (T_f) increased from 323K to 343K; the flux increased from 2.4 $kgm^{-2}h^{-1}$ to 15.9 $kgm^{-2}h^{-1}$ at the cold water (permeate side) temperature of 288K. As the T_f increased; the driving force across the membrane increased; thereby the permeate flux increased. According to the Antoine equation (9), the vapor pressure of the feed solution increases exponentially with the temperature and leads to an increase in the vapor pressure difference across the membrane. Therefore; the flux increased significantly as T_f increased. Now; considering the T_f at a constant value of 343K and increasing the cold water temperature on the permeate side from 288K to 303K; the flux decreased from 15.9 $kgm^{-2}h^{-1}$ to 11.2 $kgm^{-2}h^{-1}$ (see Figure 2). This is due to; as the temperature of cold water increased; resulted in the decrease of the vapor pressure difference across the membrane and hence the flux decreased.

The membrane distillation coefficient ($D_m = (1/R_v) + (1/(R_p + R_m))$) is also affected by the feed inlet temperature. As shown in the Figure 3; D_m increased from $5.45*10^{-9}$ $kgm^{-2}s^{-1}Pa^{-1}$ to $7.06*10^{-9}$ $kgm^{-2}s^{-1}Pa^{-1}$ by increasing feed inlet temperature from 323K to 338K. This change is due to the decrease in the poiseulle flow resistance (R_p). The contribution of poiseulle flow D_m is shown in Figure 3. The Poiseulle flow depends on the interfacial temperatures (T_1 and T_2); and the vapor pressure of feed and permeate on membrane surface (P_1 and P_2). By increasing the feed inlet temperature; P_m and T_m increase but the change in P_m is more than T_m as P_m increases exponentially due to change in vapor pressures p_1 and p_2. When compared to the combined resistance offered by Knudsen flow (R_k) and molecular diffusion (R_m); the resistance offered by Poiseulle flow (R_p) is less and its contribution to membrane distillation coefficient is more as shown in Figure 3. When the T_f increased from 323K to 338K; the resistance due to Poisuelle flow decreases;

Table 2: Experimental data and theoretical results used for estimating membrane parameters.

V_f (m/s)	T_f(K)	$J_{v;\,expt}$ kg/m²h) (experiment)	$J_{v;\,theo}$ (kg/m²h) (prediction)	$E_{J_v} = (1-\frac{J_{v,theo}}{J_{v,expt}})\times100$
0.2	333	6.1	6.4184	4.9607
0.4	333	7.4	7.0325	-5.3608
0.6	333	8.0	7.6284	-4.8707
0.8	333	8.4	8.2333	-2.0251
1.0	333	8.5	8.8380	3.8242

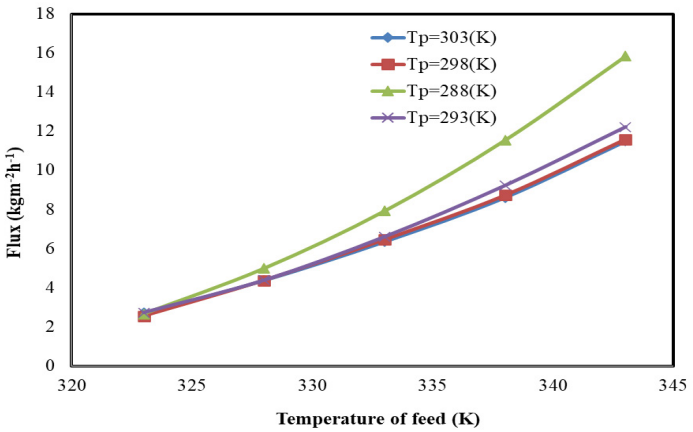

Figure 2: Effect of feed and cold water inlet temperature on the flux (v_f=0.28 m s^{-1}; v_p =0.28m s^{-1})..

thereby; this results in the increase in D_m. Resistances due to R_k and R_m are unaffected by the change in feed temperatures.

Influence of feed flow rate: Figure 4 shows that as the mass flow rate of feed (m_f) increased from 0.055 kgs^{-1} to 0.2 kgs^{-1} the flux increased from 5.14 kgm^{-2}h^{-1} to 6.6 kgm^{-2}h^{-1} at the T_f of 323K. Due to this increase in the feed velocity; there is an increase in the heat transfer coefficient on the feed side; there by the temperature polarization effect is reduced. Thus; a higher m_f increases the process driving force; resulting in higher fluxes. Along with the flow rate; increasing the feed temperature from 323K to 343K led to an increase in the flux. Considering constant inlet flow rate of 2 kg s^{-1} and increasing the T_f from 323K to 343K; the flux increased from 6.6 kgm^{-2}h^{-1} to 12.9 kgm^{-2}h^{-1} (see Figure 4).This is due to further increase in the driving force i.e. the vapor pressure difference across the membrane due to increase in the feed temperature.

By increasing the m_f from 0.01 kgs^{-1} to 0.075 kgs^{-1} increased the Temperature Polarization Coefficient $\left(TPC = \frac{T_1 - T_2}{T_f - T_p}\right)$ from 0.5257 to 0.8157; as shown in the Figure 5. As m_f increased; the turbulence on the feed side increased; and the heat transfer coefficient on feed side (h_f) increased. Due to this; the driving force; i.e; the transmembrane temperature difference (T_1 -T_2) increases; thereby increasing the TPC at higher feed flow rates. By keeping m_f constant at 0.01 kgs^{-1} and changing the T_f from 333K to 353K; the mean TPC decreased from 0.5792 to 0.5257 (Figure 5). As the T_f increased; there will be an exponential rise in the transmembrane vapor pressure (p_1-p_l); which makes the permeate flux to increase substantially. These larger permeate fluxes lead to increase in the heat fluxes through the liquid phases on feed side and permeate side; thereby increasing the temperature difference in the boundary liquid layers (feed and permeate). This resulted in an increase of the temperature polarization and a decrease of TPC (σ). Now; considering the m_f as 0.075 kg s^{-1}; TPC decreases slightly in comparison to the case of low h_f of 0.01 kg s^{-1}. This is due to the increase in the h_f at higher m_f with increase of the temperature polarization at higher temperatures got balanced.

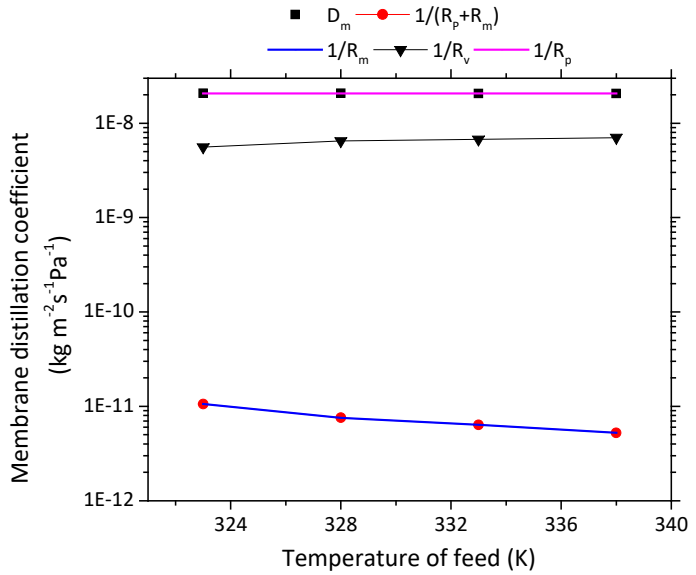

Figure 3: Influence of feed inlet temperature on membrane distillation coefficient (v_f = v_p = 0.28 m/s; T_p =298K).

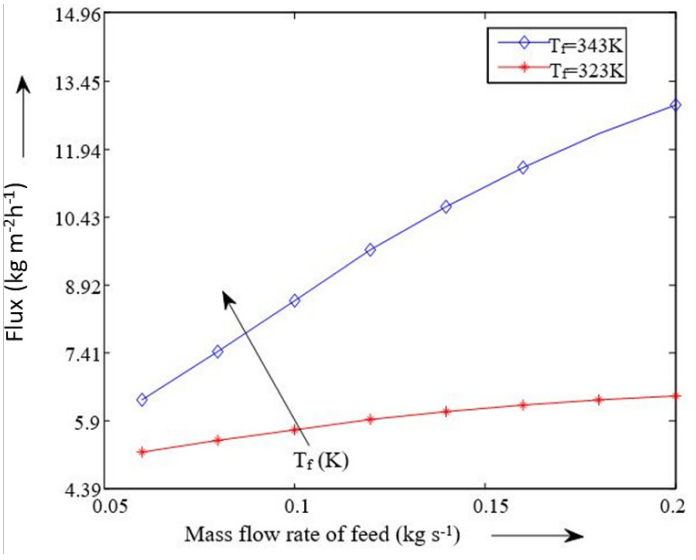

Figure 4: Influence of mass flow rate of feed on flux (=0.027 kgs^{-1};=298K).

Effect of module dimension: By increasing the membrane area of hollow fiber module leads to increase in fluxes. The membrane area is increased by increasing the length of module (L). From Figure 6 it can be seen that as the membrane length increased from 0.2 m to 0.5 m the permeate flux increased from 4.5 kg m^{-2}s^{-1} to 5.6 kg m^{-2}s^{-1}. An increase in the membrane length creates more membrane surface area which increases the average permeate flux along the length of module. Nevertheless; predictions shows that further increase in the length of module from 0.5 m to 0.8 m; resulted in decrease of average permeate flux from 5.6 kgm^{-2}s^{-1} to 5 kgm^{-2}s^{-1}. This is due to the significant decrease in the transmembrane temperature difference (T_1 -T_2) after certain length of module which resulted in decrease of the average permeate flux for the whole module.

Performance ratio evaluation

The performance ratio determines the energy efficiency of the process. In MD; one of the reasons for decrease in the driving force is due to the conductive heat losses of the membrane. Higher the conductivity of the membrane; higher is the energy transfer across the membrane and this leads to decrease in the transmembrane temperature differences. Due to this; there will be decrease in the transmembrane vapor pressure difference; which leads to decline in the flux. Membrane thickness influences the performance ratio and flux. Figure 7 shows the performance ratio (Eq. 12) with respect to the membrane thickness of the membrane. It can be observed that increase in the membrane thickness from 5 μm to 15 μm leads to decline in the flux from 15.07 kgm^{-2}h^{-1} to 2.4 kgm^{-2}h^{-1}. Due to the additional mass transfer resistance induced in the

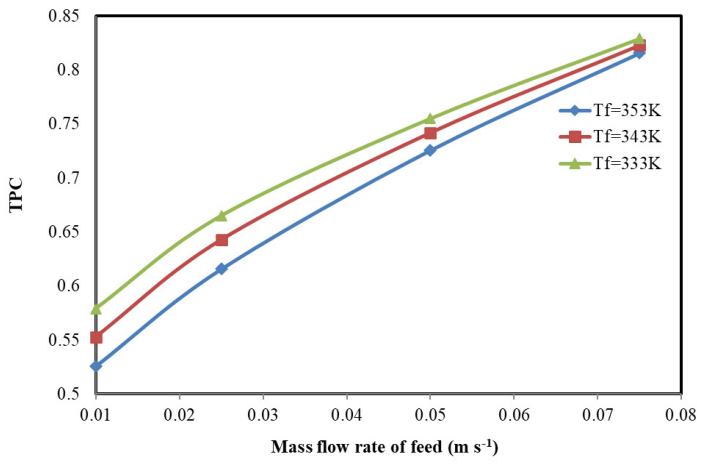

Figure 5: Influence of mass flow rate of feed on TPC (σ) (=0.027 kg s^{-1}; =298K).

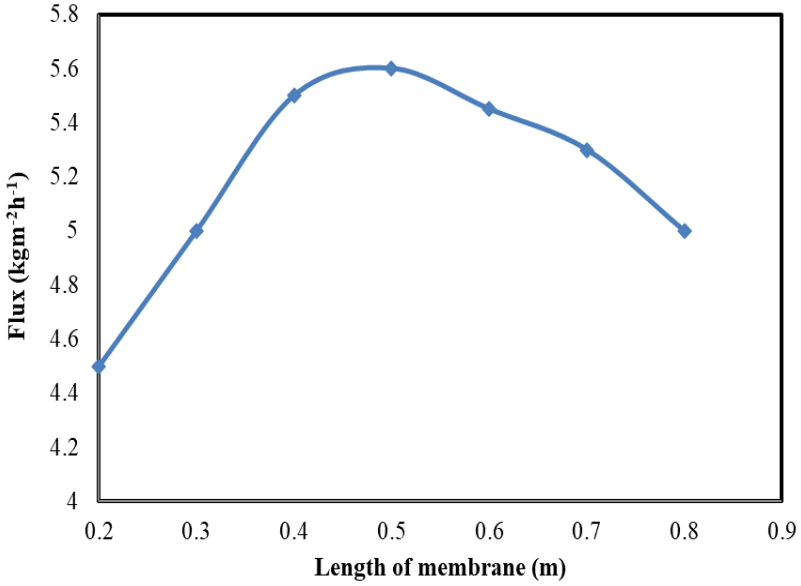

Figure 6: Effect of module length on flux (=0.055 kg s^{-1}; =0.027 kg s^{-1}; =328K; =298K)..

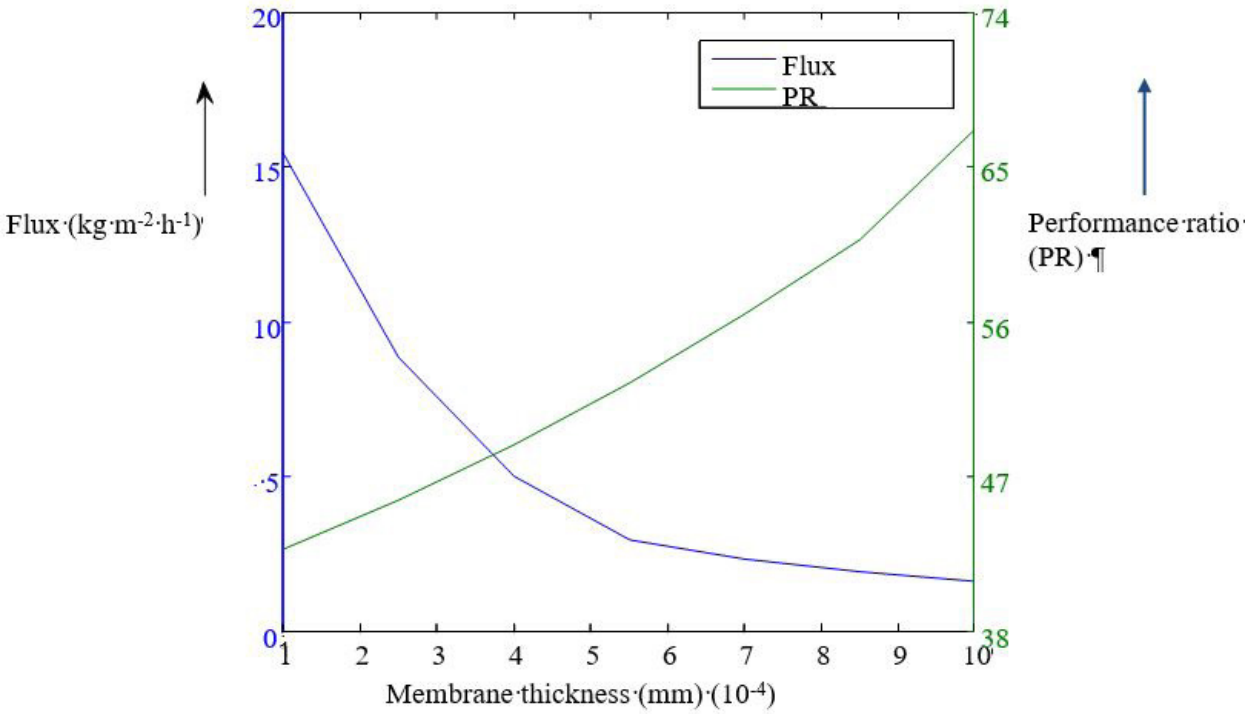

Figure 7: Effect of membrane thickness on flux and performance ratio (=0.055 kg s-1; =0.027 kg s-1; =343K; =288K)..

form of membrane thickness; the flux declines. On the other hand; increase in the membrane thickness increased the performance ratio from 40.3% to 67.25%. This is due to the additional conductive resistance induced by membrane thickness. Increase in membrane thickness leads to increase in the conductive resistance; which leads to decrease in the heat losses due to conduction of the membrane. Thus; the performance ratio increased (Figure 7). Therefore; the trade-off present between membrane thickness; flux; performance ratio should be optimized in order to achieve good thermal efficiency of the process.

SUMMARY AND CONCLUSION

- The direct contact membrane distillation model for hollow fiber modules; where the feed flows in tube side was simulated for a variety of operating conditions. The following conclusions can be drawn from the present work.
- In order to validate the model results with experimental data in literature the membrane parameters porosity (ε) and tortuosity (τ) were adjusted and are estimated from the experimental data [5]. The predicted values of membrane parameters are ε=0.73; τ=1.8. Results show that the temperature polarization coefficient remains constant along the length of module due to countercurrent flow pattern.
- The permeate flux increases significantly with change in operating parameters of feed inlet temperature and feed flow rate. On the other hand the flux decreases by increasing the permeate inlet temperature. This is due to the decrease in the driving force; which leads to reduction in the permeate flux. By increasing the membrane length; the membrane area is increased due to which the flux increased. After a certain

increase in length; the mean flux decreased due to significant decrease in the transmembrane temperature difference.

- The thermal efficiency of the membrane is analyzed through the performance ratio. Decreasing the membrane thickness increased the performance ratio; but the flux also decreased. The membrane thickness needs to be optimized for better performance ratio and at the same time to get the maximum permeate flux.

REFERENCES

1. Manyele SV, Zhu JX, Khayat RE, Pärssinen JH. Analysis of the chaotic dynamics of a high-flux CFB riser using solids concentration measurements. China Particuol. 2006;4:136-146.
2. Hsu ST, Cheng KT, Chiou JS. Seawater desalination by direct contact membrane distillation. Desalin. 2002;143(3):279-287.
3. Tomaszewska M, Gryta M, Morawski AW. Study on the concentration of acids by membrane distillation. J Memb Sci. 1995;102:113-122.
4. Garcia-Payo MC, Izquierdo-Gil MA, Fernández-Pineda C. Air gap membrane distillation of aqueous alcohol solutions. J Memb Sci. 2000;169(1):61-80.
5. Al-Obaidani S, Curcio E Macedonio F, Di Profio G, Al-Hinai H, Drioli E. Potential of membrane distillation in seawater desalination: thermal efficiency; sensitivity study and cost estimation J Memb Sci. 2008;323(1):85-98.
6. Kim YD, Thu K, Ghaffour N, Ng KC. Performance investigation of a solar-assisted direct contact membrane distillation system. J Memb Sci. 2013;427:345-364.
7. Qtaishat MR, Banat F. Desalination by solar powered membrane distillation systems. Desalin. 2013;308:186-197.
8. Duong HC, Chivas AR, Nelemans B, Duke M, Gray S, Cath TY, et al. Treatment of RO brine from CSG produced water by spiral-wound air gap membrane distillation-A pilot study. Desalin. 2015 ;366:121-129.
9. Cheng LH, Wu PC, Chen J. Modeling and optimization of hollow fiber DCMD module for desalination. J Membra Sci. 2008;318(1-2):154-166.
10. FA Banat, J Simandl. Membrane distillation for dilute ethanol: separation from aqueous streams. J Membr Sci. 1999;163(2):333-348